Deuteron NMR in solid D-T

G. W. Collins, E. M. Fearon, E. R. Mapoles, R. T. Tsugawa, and P. C. Souers
Lawrence Livermore National Laboratory, University of California, Livermore, California 94550

P. A. Fedders
Department of Physics, Washington University, St. Louis, Missouri 63130
(Received 9 September 1991)

The longitudinal relaxation times T_1 of the deuteron in solid deuterium-tritium (D-T) were measured from 2.5 to 5.0 K. They are shown to obey the Moriya-Motizuki equation, which means that relaxation takes place through the entirety of the $J=1$ D_2 line. The total $J=1$ D_2 plus $J=1$ T_2 concentrations varied from 26% to 0.75%. The D-T relaxation times were shown to be independent of the NMR frequency. The inherent relaxation times T_{11} of the D-T were in agreement with those of the deuteron in solid D_2. It was shown that the deuteron T_{11} values could be derived from those of the proton by adjusting the d term of the Hamiltonian. In contrast, the deuteron data for HD in the literature does not obey the Moriya-Motizuki equation, and the derived T_{11} values are much larger than those of D_2 and D-T. It was postulated that electric-field gradients from molecular size mismatches in the crystal cause restricted spin diffusion and a diffusion coefficient on the order of 10^{-17} m^2/s was calculated.

I. INTRODUCTION

For many years, we have studied the nuclear magnetic resonance (NMR) of the triton in solid deuterium-tritium (D-T). The triton is magnetically similar to the proton. Both are invisible to NMR in the $J=0$ ($I=0$) state and visible only in the $J=1$ ($I=1$) state.[1] Using the free induction decay (FID) and the longitudinal relaxation time T_1, we measured the $J=1$-to-0 (ortho-para) conversion time constants. These were shown to be determined by the concentration and diffusion of hydrogen atoms created by the tritium radioactivity.[2,3]

The relaxation times T_1 of protons and tritons in solid hydrogen at about 4.2 K are well described by the "heat capacity" theory of Moriya and Motizuki.[4] This theory worked so well for the triton in solid D-T (actually 25% D_2– 50% DT–25% T_2) that triton relaxation times were used to derive $J=1$-to-0 (para-ortho) time constants for D_2.[3] Using these conversion times, the steady-state $J=1$ D_2 concentration of 0.25% was calculated in solid D-T at 5 K and below. This value represents the residual $J=1$ D_2 present at steady state as the $J=1$-to-0 conversion balances the creation caused by the tritium radioactivity.

The triton NMR yielded a surprising amount of deuteron information, but to obtain deuteron relaxation times, it is necessary to go to deuteron NMR itself. The deuteron is more complex than the triton because it is NMR active in both rotational states. The $J=1$ D_2 has a nuclear spin of $I=1$, but the $J=0$ D_2 is made up of $\frac{1}{6}$ $I=0$ and $\frac{5}{6}$ $I=2$ states. In addition, the deuteron has a quadrupole moment which can interact with electric-field gradients in the solid.

II. RELAXATION TIMES IN THE LITERATURE

The Moriya-Motizuki theory is the mainstay of relaxation studies in solid hydrogen.[4] This theory applies to the hexagonal-close-packed phase, i.e., to 0.5 K for low $J=1$ samples, but somewhere around 2 to 4 K for high $J=1$ samples. The theory also fails when thermal diffusion of the molecules becomes large, somewhere above 10 to 12 K.

The theory is summarized by the schematic of energy flow in Fig. 1. Consider the case of protons in HD, the most magnetically similar molecule to DT. All HD contains impurity level concentrations of H_2, and these determine the relaxation times. The HD proton magnetic energy flows to the $J=1$ H_2 nuclei with a spin diffusion time constant T_{1c}. The $J=1$ H_2 nuclei then pass the energy to the $J=1$ H_2 molecular rotation with the "inherent" relaxation time T_{11}. For protons, $T_{11} \ll T_{1c}$. The rotations then pass the energy quickly to the crystal lattice. The $J=0$ H_2 molecules have no nuclear spin and are neutral in this theory.

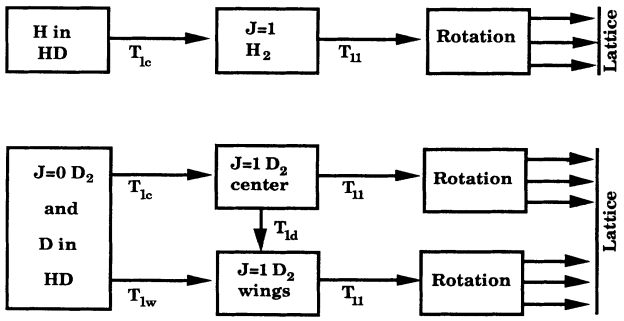

FIG. 1. Schematic flow of nuclear magnetic energy in longitudinal relaxation of the solid hydrogens by the EQQ mechanism. The top figure schematically shows proton relaxation in HD containing H_2. The bottom figure shows relaxation of HD or $J=0$ D_2 deuterons in D_2 or HD containing $J=1$ D_2.

Associated with the Moriya-Motizuki theory for solid hydrogen is the electric quadrupole (EQQ) theory.[5] The EQQ theory of nuclear relaxation states that the electric quadrupoles of nearby $J=1$ molecules interact and split the $J=1$ energy level into a band, at least at high $J=1$ concentrations. When transitions in this band are comparable to the NMR frequency, nuclear relaxation occurs via the T_{1l} channel. This "spin-rotation" relaxation short circuits the usual spin-lattice relaxation, which is much longer and is not shown in Fig. 1. This effect is expected to be independent of both temperature and the magnetic field. The EQQ band theory predicts a relaxation time that is independent of temperature and NMR frequency on the high-concentration side of the T_1 minimum.

We may elaborate by considering the Hamiltonian for an isolated hydrogen molecule in a strong dc magnetic field. The first two terms describe the Zeeman interaction of the nuclear and rotational magnetic moments with the magnetic field. The next terms describe the nuclear-rotational and nuclear-nuclear coupling that will create relaxation. The part of the Hamiltonian H_{cd} is given by[6,7]

$$h^{-1}H_{cd}=-c\mathbf{I}\cdot\mathbf{J}-5d[3(\mathbf{I}_1\cdot\mathbf{r}/r)(\mathbf{I}_2\cdot\mathbf{r}/r)-\mathbf{I}_1\cdot\mathbf{I}_2]\ , \tag{1}$$

where c and d are constants, and I_1 and I_2 are the individual nuclear spins on the atoms. These constants were measured in molecular beam measurements by Ramsey[6] and are H_2 $c=113.8$ KHz, $d=57.68$ KHz; D_2 8.783 and 25.24 kHz. The molecular beam work on isolated molecules was then carried over to the dense gas, where Lipsicas and Bloom report Schwinger's calculated relaxation time of[8]

$$\frac{1}{T_1}=\left[\frac{4c^2}{3}+15d^2\right]\tau_1\ , \tag{2}$$

where τ_1 is the time spent by $J=1$ molecules in a given m_J substate. For Eq. (2) to be valid, $1/\tau_1$ should be much smaller than the NMR frequency. Actually, the c and d terms each have their own frequency distributions, so that equating them is necessary in order to achieve the single m_J-hopping time in Eq. (2). Because the hydrogen molecule rotates freely in the solid, Eqs. (1) and (2) were taken directly into the theory of solid H_2 by Fuijo, Hama, and Nakamura[9] and Ebner and Myles.[10] In H_2, $T_1=T_{1l}$, so that we shall take Eq. (2) as a description of T_{1l}.

We return to consider Fig. 1. For protons in HD, $T_{1c}\ll T_{1l}$, so that the HD and $J=1$ H_2 impurities have the same spin temperature and show a single FID. However, all energy still funnels through the $J=1$ H_2, so that it is the bottleneck in the process. The strong coupling of the two kinds of hydrogen leads to the Moriya-Motizuki equation:

$$T_1\ (\text{H in HD})=\frac{2[J=1\ H_2]+\frac{3}{4}[\text{HD}]}{2[J=1\ H_2]}T_{1l}\ , \tag{3}$$

where the quantities in brackets are the mol % of the species. The sum of all hydrogen percents in this paper will add up to 100%. The numbers are equal to $I(I+1)$. The bracketed terms, then, represent the nuclear magnetic heat capacities, and all energy funnels through the $J=1$ H_2 molecules in the denominator. All EQQ information is included separately in T_{1l}. The transfer of nuclear magnetic energy may be made to any $J=1$ species because the electric molecular quadrupole moments of all $J=1$ hydrogens have the same size. Thus T_{1l} will be a function of the sum of the $J=1$ species, and this fact was used earlier to determine the $J=1$-to-0 D_2 time constants from triton T_1's.[3]

The Moriya-Motizuki theory is expected, then, to produce the same value of the proton T_{1l} in H_2 (where $T_1=T_{1l}$) as in HD. We have already noted that this is true,[11] but it is so important that we show the full set of literature 4.2-K data in Fig. 2. The H_2 data are taken from Buzerak, Chan, and Meyer,[12] and it includes data by Hardy and Gaines,[13] Weinhaus and Meyer,[14] and Gaines, Chi, and Constable.[15] The published HD data are partly from Hardy and Gaines,[13] but most are unpublished work by Mano.[16] We include his data on proton T_1's taken by doping with $J=1$ D_2. The T_{1l}'s were obtained by using in Eq. (1) the very low residual concentrations of $J=1$ H_2 that were obtained after waiting for weeks for $J=1$-to-0 catalysis. We expect that a common T_{1l} curve should be present as a function of total $J=1$ concentration, regardless of the isotope that creates the $J=1$ state. We find that this is true, so that Fig. 2 should be taken as confirmation of the Moriya-Motizuki theory with the strong coupling of the two kinds of hydrogens.

We shall now apply the Moriya-Motizuki theory for the deuteron in solid D_2 and HD. From the proton relaxation diagram in Fig. 1, we expect the $J=0$ D_2 and HD to relax through the $J=1$ D_2. For strong coupling, we expect all magnetic energy to flow through the T_{1c} channel with $T_{1c}\ll T_{1l}$. Then, we obtain

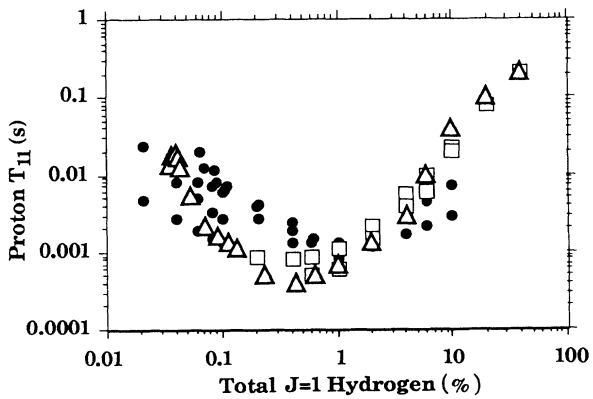

FIG. 2. Inherent relaxation times at 4.2 K, T_{1l} (in s), for protons in H_2 and HD, showing that they are in agreement. The samples are H_2 (□), HD with $J=1$ H_2 being added (△), and HD with $J=1$ D_2 being added (●). The sum of $J=1$ H_2 plus $J=1$ D_2 is plotted on the x axis. The NMR frequencies are H_2 top 5–30 MHz, H_2 bottom 4–5 MHz, and all HD 60 MHz. The closed triangles far to the left probably represent an error in the $J=1$ concentration.

$$T_1\ (J=0\ D_2 \text{ in } D_2)=\frac{5[J=0\ D_2]+2[J=1\ D_2]}{2[J=1\ D_2]}T_{11}\ . \tag{4}$$

In nD_2, $[J=0\ D_2]=100-[J=1\ D_2]$ so that

$$T_1\ (J=0\ D_2 \text{ in } D_2)=\frac{500-3[J=1\ D_2]}{2[J=1\ D_2]}T_{11}\ . \tag{5}$$

This is the form usually encountered in the literature. The strong-coupling case in HD likewise becomes

$$T_1(\text{D in HD})=\frac{2[\text{HD}]+5[J=0\ D_2]+2[J=1\ D_2]}{2[J=1\ D_2]}T_{11}\ . \tag{6}$$

With nD_2 being added as the dopant, $[J=0\ D_2]=2[J=1\ D_2]$ so that

$$T_1\ (\text{D in HD})=\frac{100+3[J=1\ D_2]}{[J=1\ D_2]}T_{11}\ . \tag{7}$$

Now, the strong-coupling model is known to be too simple in D_2. Harris predicted that the $J=1$ D_2 and $J=0$ D_2 would be decoupled.[17] This was confirmed in the Meyer laboratory, where it was found that the $J=1$ D_2 line was broadened inhomogeneously at least an order of magnitude wider than expected by dipole-dipole interaction.[18–20] Two longitudinal relaxation times were found: a long one representing mainly $J=0$ D_2 and a short one representing $J=1$ D_2. The long one was the one almost universally measured before, because it was easy to see. The two signals could not be totally ascribed to the two species of D_2, and it appeared there was some kind of mixing between them.

The Meyer group suggested a two-bath model of $J=0$ D_2 relaxation, which we shall simplify schematically in Fig. 1. For fast $J=1$ relaxation (so that it does not interact with the $J=0$ system), we would expect

$$T_1(J=1\ D_2 \text{ in } D_2)\simeq T_{11}\ . \tag{8}$$

Strong coupling would occur in Fig. 1 for $T_{1w}\simeq T_{1c}\ll T_{11}$. However, Meyer and co-workers suggested that the narrow line $J=0$ D_2 could relax to the broad line $J=1$ D_2 only in the small fraction (about 10%) where overlap of the two NMR lines occurred. In Fig. 1, we could then consider the T_{1w} channel to be blocked, and two new times could be added. The time T_{1c} would represent a spatial spin diffusion time for a $J=0$ molecule to find a $J=1$ molecule to relax with. The time T_{1d} would represent a spectral diffusion time in frequency space, i.e., the diffusion of nuclear magnetic energy from the center of the $J=1$ line to the wings. We note that for T_{1c}, $T_{1d}<T_{11}$ we obtain

$$T_1(J=0\ D_2 \text{ in } D_2)\simeq\frac{5[J=0\ D_2]T_{11}}{2[J=1\ D_2]}\ . \tag{9}$$

This is almost the same as the strong-coupling case of Eq. (4), and it would be experimentally indistinguishable in experiments using low percentages of $J=1$ D_2.

Before we turn to the literature data, we first reconsider what T_{11} should be for the deuteron. We have T_{11} values for the proton in H_2 down to 0.1% $J=1$ H_2 and HD data down to about 0.002%.[21] We use these to calculate T_{11} for the deuteron using Eq. (2). We obtain

$$T_{11}(D_2)/T_{11}(H_2)=(4c^2/3+15d^2)_{H_2}/(4c^2/3+15d^2)_{D_2}\simeq 7\ . \tag{10}$$

We average the H_2 and HD data and multiply by 7 to obtain these empirical deuteron equations:

$$T_{11}(D_2)\simeq 0.0041+0.005\{[J=1]-0.4\}^{1.55}\ ,\quad 0.4 \text{ to } 40\%\ J=1 \tag{11}$$

and

$$T_{11}(D_2)\simeq 0.0036+0.00014[J=1]^{-1.35}\ ,\quad 0.002 \text{ to } 0.4\ \%\ J=1\ , \tag{12}$$

where $[J=1]$ refers to the total $J=1$ species and a magnetic field of about 1 T is implied. The T_{11} minimum occurs at 0.4%.

We now turn to the literature and calculate T_{11} (strong) for the various deuteron cases using Eqs. (5), (7), and (8). All were measured at NMR frequencies from 2.6 to 6.2 MHz. The data used for $J=0$ D_2 from 1.2 to 4.2 K were taken by Honig *et al.*,[22] Wang, Smith, and White,[23] and Meyer and co-workers.[18–20] The $J=1$ D_2 data are taken from Calkins *et al.*[24] The HD data are again all taken from the unpublished work of Mano, where both $J=1$ D_2 and $J=1$ H_2 were used as dopants.[16] The results are shown in Fig. 3, again plotted against the total $J=1$ concentration.

There is a lot of important information in Fig. 3, and we shall first consider the well-behaved $J=0$ D_2 data. These results fall on the expected deuteron lines for $J=1$ concentrations down to about 0.2%. This means that the strong-coupling model [at least in the version of Eq. (9)] works for $J=0$ D_2 even though there may be a decoupled $J=1$ species. Also, the placement of the short $J=1$ D_2 data on the same line offers encouragement that this is, indeed, a direct measure of T_{11}.

However, Fig. 3 shows an effect that we believe has not been noticed in the literature: that there are two different T_1 (strong) curves for D_2 and HD. We have already shown that the D_2 curve is that expected by an EQQ extrapolation of proton data. Therefore some unexpected mechanism is at work in HD to lengthen the relaxation times. We even have a recent confirmation by Ganem and Norberg,[25] who measured deuteron T_1's at 55 MHz at the higher temperatures of 8–11 K in mixtures of HD and nD_2. In Fig. 3, their data are shown by the circles. We note that four points lie on the D_2 curve, three on the HD curve, and one in between. Their points on the D_2 curve range from pure nD_2 to mixtures of nD_2 with HD up to 88%. The sample in between the curve has a composition of 90% HD–10% nD_2. All samples on the HD

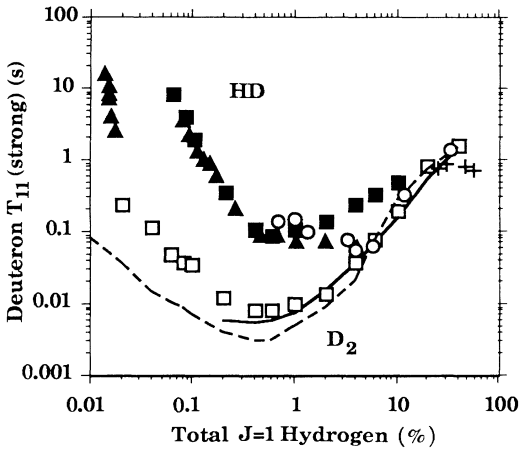

FIG. 3. Inherent relaxation times T_{11} (strong) (in s), as calculated for deuteron data in solid hydrogen, clearly showing the existence of two separate curves: one for HD (▲ , ■) and one for $J=0$ D_2 (□). Calculated T_{11} curves using Eq. (10) are shown as derived from protons in H_2 (——) and HD (— — —), showing that $J=0$ D_2 obeys the EQQ theory down to about 0.2% $J=1$. The $J=1$ D_2 T_1 data (+) falls on the D_2 curve as expected. The Ganem and Norberg data (○) unexpectedly crosses from the D_2 line to the HD line. The HD data include doping with $J=1$ D_2 (□) and $J=1$ H_2 (▲). The mismatch in data at the left illustrates the uncertainties in working at low $J=1$ concentrations. All samples were measured at 2.6–6.2 MHz, except the Ganem and Norberg data at 55 MHz.

curve contain 96% HD or more, with the remainder being D_2. There are two Mano and Honig points (black triangles, one hidden behind a circle) in between the D_2 and HD curves, which confirm the Ganem and Norberg results.

These considerations are important because we are about to consider D-T measurements without having resolved the difference in behavior between D_2 and HD. All of the Mano-Honig measurements on HD were surely on the $J=0$ line.[26] No one has yet looked at the $J=1$ D_2 line in HD to find out why the T_1 (long) values are an order of magnitude longer than expected. Nor were we able to see a short-T_1 component in our D-T work, so that models of T_{11} become of considerable importance.

III. EQUIPMENT AND PROCEDURE

The measurements were made with a pulsed NMR spectrometer at 5.8–7.0 MHz, with a few at 26 and 52 MHz. The $\pi/2$ times ranged from 8 to 18 μs. The linewidths will be described in an upcoming paper,[27] and we shall summarize their properties here. The deuteron species with long transverse relaxation times T_2 had these approximate values: $J=0$ D_2 in D_2 590 μs, D in HD 480 μs, and D in D-T 330 μs. The corresponding linewidths were 0.9, 1.1, and 1.6 kHz, respectively. The above free-induction decays were so long that the 20-μs receiver dead time was not important. We did observe $J=1$ D_2 in D_2 with a 50-μs relaxation time and an 11-kHz linewidth. This difficult signal was not seen in HD or D-T, but the amounts of $J=1$ D_2 were probably too low. The longitudinal relaxation times were measured by the saturation caused by $\pi/2$ pulse trains. The T_1 decay is given by

$$1-S/S(0)=\exp(-t/T_1)\ . \tag{13}$$

The exponential nature of all the T_1 decays is illustrated in Fig. 4. The sample size was about 5.5 mmol in a sapphire tube of 2 mm radius. The correction needed for the radioactive decay heat of tritium decay has been discussed previously.[3] It amounts to 0.1 K at 2 to 3 K and no change at 5 K and higher.

Most runs were made with equilibrium D-T. One sample, however, was enriched DT made by the chemical reaction of lithium tritide and deuterated methyl alcohol.[28] We did not have direct analysis of this sample but used the average from the five earlier runs with the connecting tubes at room temperature: 87% DT, 6% D_2, 2.5% T_2, 2.5% HD, and 2% HT.

The $J=1$ concentrations were calculated using the temperatures, times, and the $J=1$-to-0 time constants τ_J previously determined.[3] For $J=1$ D_2 in equilibrium D-T, the behavior would be described by

$$[J=1\ D_2]=\{[J=1\ D_2]_0-0.25\}\exp(-t/\tau_J)+0.25\ , \tag{14}$$

where $[J=1\ D_2]_0$ is the time-zero concentration and 0.25 is the steady state $J=1$ D_2 concentration. The time constant τ_J is about 5 h for both $J=1$ D_2 and $J=1$ T_2 at 5 K and below. The $J=1$ T_2 obeys the same equation, but with a 0.5% steady-state end point.

The concentrations in the enriched DT must be calculated with a model. First, the various species are produced in a nonequilibrium mix. They react to the 25% D_2-50% DT–25% T_2 mix with a time constant τ_{ex} of 200 h. The molecular DT will change approximately as

$$[DT]=50+\{[DT]_0-50\}\exp(-t/\tau_{ex})\ , \tag{15}$$

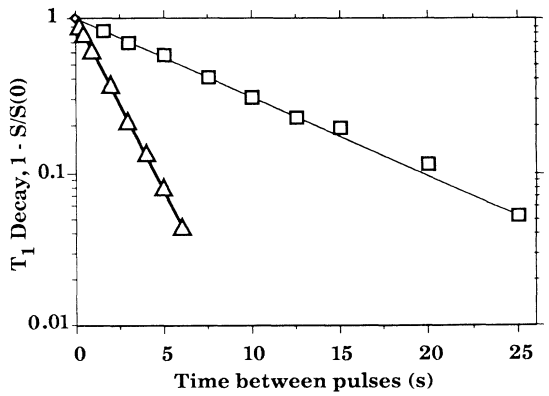

FIG. 4. T_1 decay function for deuterons in solid D-T at 3.5 K, showing the exponential character of the decay. The samples are 1.6 h old, with 4.5% $J=1$ D_2 and 9.5% $J=1$ T_2 (□); and 22 h old, with 0.3% $J=1$ D_2 and 0.7% $J=1$ T_2 (△).

and the D_2 and T_2 will change according to

$$[D_2]=[D_2]_0+\{25-[D_2]_0\}[1-\exp(-t/\tau_{ex})] . \quad (16)$$

We neglect the small amounts of HD and HT. The $J=1$ species are to be found using the rate equations[3,29]

$$d[J=1\ D_2]/dt=-[J=1\ D_2]/\tau_J + (1/6\tau_{ex})\{[D_2]+[DT]/2\} \quad (17)$$

and

$$d[J=1\ T_2]/dt=-[J=1\ T_2]/\tau_J + (3/8\tau_{ex})\{[T_2]+[DT]/2\} . \quad (18)$$

Equations (17) and (18) may be integrated numerically over the time of the experiment.

IV. RESULTS

The T_1 values for deuterons in D-T were monitored with time in the range 2.5–5.0 K. The same decrease, minimum, and shallow rise seen previously for tritons[11] were seen here as shown in Fig. 5. At the same time, the time-zero FID height increased slightly with time, as shown in Fig. 6. Both are expected from the known 5-h $J=1$-to-0 time constants for D_2 and T_2 at these temperatures. We would expect the FID height to increase by about 12% as the 16.7% $J=0$ D_2 in normal D-T converts to almost 25% $J=0$ D_2 in equilibrium D-T. This change in FID height is too small to make direct deuteron measurement a satisfactory way of obtaining $J=1$-to-0 time constants.

We next turn to the important determination of T_{11}, where we calculate T_{11} (strong) according to

$$T_{11}(\text{strong})=2[J=1\ D_2]T_1/\{2[J=1\ D_2]+5[J=0\ D_2] + 2([DT]+[HT])\} . \quad (19)$$

The T_{11} (strong) results are shown in Fig. 7 as a function of the total $J=1$ D_2 plus $J=1$ T_2 concentrations. We see that our D-T results lie on the D_2 line so that the use of the strong-coupling model for D-T appears reasonable. It is only the HD line that remains inexplicably high.

We also measured two deuteron frequencies in a D-T sample held at 2–4 K overnight, so that the total $J=1$ concentration was about 1%. Two T_1 measurements at 26 MHz produced 1.7 s and two at 53 MHz yielded 1.8 s. No frequency dependence was seen at 1% total $J=1$ concentration.

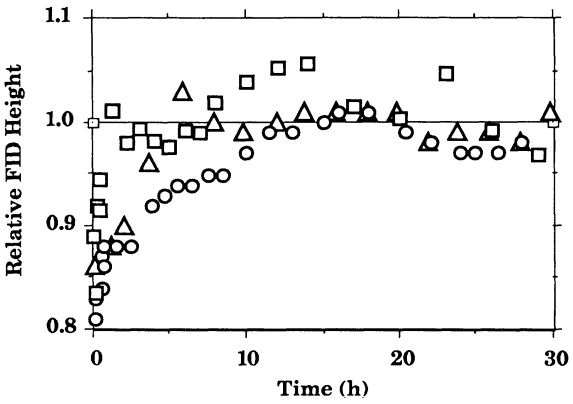

FIG. 6. Increase of the FID showing the $J=1$-to-0 conversion of the D_2 in solid D-T. The samples are 5.0 K (△); 3.5 K (○) and 2.5 K (□).

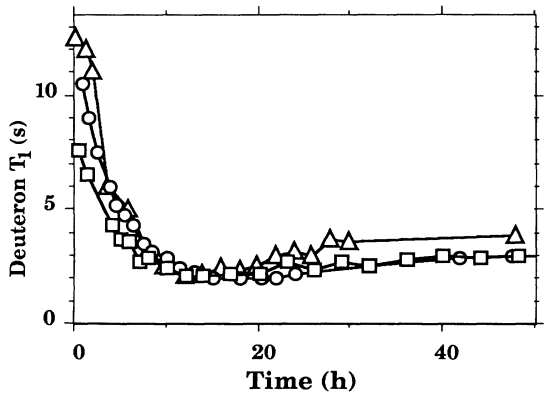

FIG. 5. Change of the measured deuteron T_1 values with time in equilibrium D-T. The samples are 5.0 K and 7.0 MHz (△); 3.5 K and 5.9 MHz (○); and 2.4–2.6 K and 5.9 MHz (□).

V. DISCUSSION

We shall consider possible mechanisms that could cause the difference in relaxation time behavior between HD, D_2, and D-T. A first question is whether the three-times-larger proton magnetic moment in HD can affect the deuterons. However, the transverse relaxation time of the protons is an order of magnitude shorter than that of the deuterons. Thus the rapid flipping of the protons effectively decouples them from the deuterons.

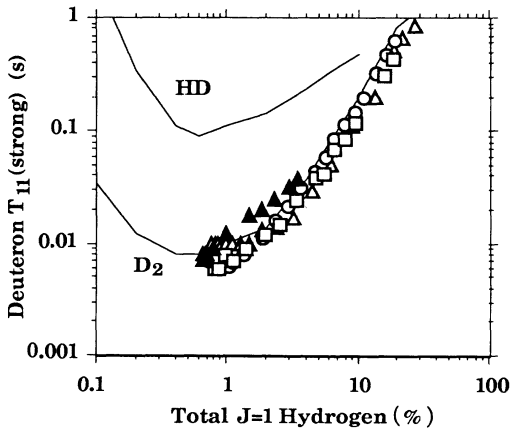

FIG. 7. Deuteron T_{11} (strong) values as calculated from the measured D-T data and compared with literature data for HD (upper line) and $J=0$ D_2 in D_2 (lower line). The strong coupling model for T_{11} is used. The D-T samples are 5.0 K (△); 3.5 K (○), and 2.5 K (□). The enriched DT sample at 4.9 K is indicated by (▲).

We suggest the possibility that lattice strains exist that create electric-field gradients and restrict the deuteron spin diffusion. We note these listed (measured and estimated) molar volumes in $\mu(m^3)$/mol at 0 K for the hydrogens $J=0$ H_2, nH_2, HD, $J=0$ D_2, nD_2, DT, and $J=0$ T_2: 23.06, 22.76, 21.37, 19.93, 19.86, 19.29, and 18.78, respectively.[30] For $J=1$ D_2, we estimate a value of 19.72 $\mu(m^3)$/mol. For a 50-50 combination of two species, we expect an alloy in which an intermediate molar volume with no lattice strains is formed. As we approach a preponderance of one species, the other becomes an impurity which is more difficult to fit into the lattice of the host. The fractional volumetric difference between $J=1$ D_2 in a $J=0$ D_2 host is -1.1%, and as seen in Fig. 3, T_{11} deviates from the expected deuteron curve for $J=1$ D_2 quantities below 0.1%. However, never does the D_2 T_{11} value rise as high as the HD line. The volumetric difference for nD_2 impurity in an HD host is a much larger -7.1%, and the anomalously long-T_{11} behavior is in effect for 4% nD_2 concentrations or less. For nH_2 in HD, the volumetric difference is $+6.5\%$ and the long-T_{11} behavior appears at about 1.3% nH_2. We recall that the D_2 work was at warmer temperatures than the H_2 work, and the mixing of the hydrogens was more carefully done in the D_2 work, so that these factors could create differences in the results.

For $J=0$ D_2 and $J=0$ T_2 in D-T, the volumetric differences are 3.3% and -2.6%, in between the HD and D_2 cases described above. We might expect that restricted deuteron spin diffusion appears at D_2+T_2 concentrations of 1% or less. Even our enriched DT contained much more than this, and all D-T samples contain about 1% each of HD and HT. We had previously suggested that superpure molecular DT would be the key to lengthening the relaxation times.[11] This was based on the need to reduce the $J=1$ species because of the basic EQQ mechanism. However, the lattice strains will be reduced by nonmagnetic $J=0$ species. To obtain the long-T_1's of the HD mechanism in D-T, we need to remove all other hydrogens as well to a low concentration.

We now return to Fig. 1 to consider the relaxation pathway for deuterons in HD. For T_{1w}, $T_{1d} \gg T_{11}$, and $T_{1c} \ll T_{11}$, we have relaxation only through the line center. Then, T_1 is lengthened by the inverse of the fraction of nuclei in the line center b. Calkins *et al.* measured this in D_2 as being 0.13 at 3 K, 0.083 at 2K, and 0.07 at 1.5 K.[24] These are not small enough to explain the 200-s T_1 in D_2 with 0.06% $J=1$ D_2 and the 14 000 s in HD with the comparable amount.[16,22]

We next consider lengthening T_{1c} and T_{1w}, which amounts to restricted spatial spin diffusion. We assume that both parts of the $J=1$ D_2 line are involved in the relaxation. This is certainly true at high $J=1$ values, where the T_{11} values for HD and D_2 are comparable. For T_{1w} long and T_{1d} short, we have

$$T_1 = QT_{1c}/b + QT_{11} , \tag{20}$$

where

$$Q = \{2[\mathrm{HD}] + 5[J=0\ D_2]\}/2[J=1\ D_2] . \tag{21}$$

Another route is to have T_{1d} long and $T_{1w}=T_{1c}$. Then we have

$$T_1 = Q(T_{1c} + T_{11}) . \tag{22}$$

Finally, we relate T_1 to the spin diffusion coefficient D by

$$D \simeq \frac{1}{4T_{1c}} \left[\frac{100}{[J=1\ D_2]} \right]^{2/3} R_0^2 , \tag{23}$$

where R_0 is the intermolecular distance (0.37 nm) (Ref. 30) and the $J=1$ molecules are assumed to be randomly dispersed.

For HD, we take experimental T_1 values and substitute T_{11} values from D_2, on the assumption that these are the true inherent relaxation times. Then, for $\beta=0.1-0.2$, Eqs. (20), (21), and (23), give, for $0.06 \leq [J=1\ D_2] < 10\%$, diffusion coefficients of 2×10^{-18} to 7×10^{-17} m^2/s. Equations (22) and (23) give a larger spread from 7×10^{-19} to 10^{-16} m^2/s. We may compare these with Fedders's calculated diffusion coefficient of[31]

$$D \simeq 1.7\times10^{-17}/\Delta\nu_n^2 , \tag{24}$$

where $\Delta\nu_n$ is the NMR linewidth in kHz. Using our measured value of 1.1 kHz, Eq. (24) produces a value of 10^{-17} m^2/s, in agreement with our simple models.

ACKNOWLEDGMENTS

We would like to thank Chris Gatrousis and Tom Sugihara of the Chemistry and Materials Science Department and John Holzrichter and John Nuckolls of the Institutional Research and Development fund for their support of this work. One of us (P.A.F.) acknowledges partial support by LLNL. This work was performed under the auspices of the U.S. Department of Energy by the Lawrence Livermore National Laboratory under Contract No. W-7405-ENG-48.

---

[1] J is the molecular rotational quantum number and I is the nuclear magnetic quantum number.

[2] J. R. Gaines, J. D. Sater, E. M. Fearon, P. C. Souers, F. E. McMurphy, and E. R. Mapoles, Phys. Rev. Lett. **59**, 563 (1987).

[3] G. W. Collins, E. M. Fearon, E. R. Mapoles, P. C. Souers, and P. A. Fedders, Phys. Rev. B **44**, 6598 (1991).

[4] T. Moriya and K. Motizuki, Prog. Theor. Phys. **18**, 183 (1957).

[5] D. A. Drabold and P. A. Fedders, Phys. Rev. B **39**, 6325 (1989).

[6] N. F. Ramsey, Phys. Rev. **85**, 60 (1951).

[7] F. Reif and E. M. Purcell, Phys. Rev. **91** 631 (1953).

[8] M. Lipsicas and M. Bloom, Can. J. Phys. **39**, 881 (1961).

[9] M. Fuijo, J. Hama, and T. Nakamura, Prog. Theor. Phys. **54**,

293 (1975).
[10]C. Ebner and C. W. Myles, Phys. Rev. B **12**, 1638 (1975).
[11]P. C. Souers, E. M. Fearon, E. R. Mapoles, J. D. Sater, G. W. Collins, J. R. Gaines, R. H. Sherman, and J. R. Bartlit, Fusion Tech. **14**, 855 (1988).
[12]R. F. Buzerak, M. Chan, and H. Meyer, J. Low Temp. Phys. **28**, 415 (1977).
[13]W. N. Hardy and J. R. Gaines, Phys. Rev. Lett. **17**, 1278 (1966).
[14]F. Weinhaus and H. Meyer, Phys. Rev. B **7**, 2974 (1973).
[15]J. R. Gaines, Y. C. Chi, and J. H. Constable, Phys. Rev. B **17**, 1028 (1978).
[16]H. Mano, Ph.D. thesis, Syracuse University, 1978. The data using $J=1$ H_2 doping were cited in Ref. 11.
[17]A. B. Harris, Phys. Rev. B **2**, 3495 (1970).
[18]F. Weinhaus, H. Meyer, and S. M. Myers, Phys. Lett. **37A**, 245 (1971).
[19]F. Weinhaus, H. Meyer, and S. M. Myers, Phys. Rev. B **7**, 2948 (1973).
[20]F. Weinhaus, S. M. Myers, B. Maraviglia, and H. Meyer, Phys. Rev. B **3**, 626 (1971).
[21]There is a sharp bend in the Mano data for H in HD in Fig. 4.1 of Ref. 16. We think it better to extrapolate the data using the results for the $[J=1\ H_2]=0.1\%$ to 0.01% range. This produces the adjusted values of $[J=1\ H_2]$ (%) and T_1 (s) of 0.008, 65; 0.006, 120; 0.004, 270; and 0.002, 1700.
[22]A. Honig, M. Lewis, Z.-Z. Yu, and S. Yucel, Phys. Rev. Lett. **56**, 1866 (1986).
[23]R. Wang, M. Smith, and D. White, J. Chem. Phys. **55**, 2661 (1971).
[24]M. Calkins, R. Banke, X. Li, and H. Meyer, J. Low Temp. Phys. **65**, 47 (1986).
[25]J. Ganem and R. E. Norberg, Phys. Rev. B **43**, 1 (1991).
[26]Bozler and Graf measured the proton T_1 HD with $J=1$ H_2 as the dopant at 50 mK and 60–429 MHz. Low $J=1$ values of 0.003 to 0.2% were studied. The data are quite scattered, but the temperature effect between these data and Honig's at 4.2 K appears to be there. A roughly linear frequency effect appears present for $J=1$ values below about 0.1%. See H. M. Bozler and E. H. Graf, J. Low Temp. Phys. II **LT-13**, 218 (1973).
[27]P. C. Souers, R. T. Tsugawa, E. M. Fearon, G. W. Collins, and P. A. Fedders (unpublished).
[28]E. M. Fearon, R. G. Garza, C. M. Griffith, S. R. Mayhugh, E. R. Mapoles, P. C. Souers, R. T. Tsugawa, J. D. Sater, G. W. Collins, and J. R. Gaines, Fusion Tech. **14**, 864 (1988).
[29]We recall that $\tau_{ex}=2/k$, where k is the hydrogen-atom production rate of $2.84\times10^{-6}\ s^{-1}$ in pure tritium. See Ref. 3.
[30]P. C. Souers, *Hydrogen Properties for Fusion Energy* (University of California, Berkeley, 1986), p. 80.
[31]P. A. Fedders, Phys. Rev. B **38**, 4740 (1988).